Pertanika J. Sci. & Technol. 33 (5): 2027 - 2047 (2025)

PERTANIKA JOURNALS

SCIENCE & TECHNOLOGY

Journal homepage: http://www.pertanika.upm.edu.my/

Using Deep Transfer Learning for Automated Identification of Susceptibility Vessel Signs in Patients with Acute Ischemic Stroke

Nur Lyana Shahfiqa Albashah[1,2]*, Ibrahima Faye[1], Fityanul Akhyar[2] and Ahmad Sobri Muda[3]

[1]Department of Fundamental and Applied Science, Universiti Teknologi Petronas, 32610 Bandar Seri Iskandar, Perak, Malaysia

[2]Faculty of Information and Communication Technology, Universiti Tunku Abdul Rahman, 31900 Kampar, Perak, Malaysia

[3]Putra Clinical Centre Neurovascular and Stroke, Hospital Sultan Abdul Aziz Shah, Faculty of Medical and Health Science, Universiti Putra Malaysia, 43400 Serdang, Selangor, Malaysia

ABSTRACT

Ischemic stroke, commonly caused by a blood clot obstructing the blood flow within brain vessels, requires accurate identification of the clot to determine appropriate treatment. Susceptibility-weighted imaging (SWI) is an imaging modality that effectively captures clots within the brain. The susceptibility vessel sign (SVS) visible on SWI images is crucial for influencing treatment outcomes. Traditionally, radiologists manually analyse the SVS, which is both challenging and time-consuming. This research aims to build an interactive deep learning (DL)-assisted method for identifying the SVS on the SWI in patients with acute ischemic stroke. Sixty-six images with SVS positive were used, and 66 images with SVS negative were used, with regions of interest extracted to create the training, validation, and test datasets. To increase the number of training samples, data augmentation was used. A deep convolutional neural network DenseNet121 was utilised to identify input images as either SVS positive or SVS negative. In terms of diagnostic performance using 5-fold cross validation, the DenseNet121 model achieved 96.92% sensitivity, 92.31% specificity, and 94.64% accuracy on the test dataset. These findings indicate that the DL methods might be advantageous for detecting the SVS on the SWI in patients with acute ischemic stroke.

Keywords: Brain stroke, DenseNet model, susceptibility vessel sign (SVS), SWI-MRI, transfer learning

ARTICLE INFO

Article history:
Received: 15 August 2024
Accepted: 29 April 2025
Published: 11 August 2025

DOI: https://doi.org/10.47836/pjst.33.5.01

E-mail addresses:
yanashahfiqa88@gmail.com (Nur Lyana Shahfiqa Albashah)
Ibrahima_faye@utp.edu.my (Ibrahima Faye)
fityanul@utar.edu.my (Fityanul Akhyar)
asobri@upm.edu.my (Ahmad Sobri Muda)
* Corresponding author

e-ISSN: 2231-8526

INTRODUCTION

Stroke is a severe medical condition that significantly impacts patients, both in terms of health and economic burden, especially during post-treatment care. Stroke survivors often require extensive and costly rehabilitation. Strokes can be categorised into two types: ischemic and hemorrhagic, with ischemic strokes accounting for approximately 85% of all cases (Sirsat et al., 2020). Ischemic strokes occur when a blockage obstructs a blood vessel in the brain, leading to oxygen deprivation and subsequent cell death. This results in functional impairments and delayed recovery. Therefore, rapid restoration of oxygen supply and minimisation of brain damage are crucial. In this context, brain imaging plays a vital role in diagnosing stroke types and guiding treatment strategies.

Magnetic resonance imaging (MRI) and computed tomography (CT) scans are commonly used for stroke diagnosis. Advanced imaging modalities, such as susceptibility-weighted imaging (SWI) and diffusion-weighted imaging (DWI), provide more precise localisation and assessment of the affected brain areas. The SWI, in particular, is highly effective in detecting small changes in magnetic properties between blood and tissue, enabling the identification of affected veins due to increased deoxygenated blood. Recent studies have reinforced the importance of the SWI in detecting thrombi, as the susceptibility vessel sign (SVS) has been linked to various stroke parameters, including risk factors and thrombus length, which are crucial for treatment planning.

Despite their advantages, existing brain imaging techniques have limitations. The perfusion-weighted imaging (PWI) requires contrast agents, which are unsuitable for patients with renal insufficiency. The DWI can be time-consuming and impractical for certain patients. The computed tomography angiography (CTA) is also prone to inaccuracies, such as false negatives due to vessel wall calcification and partial volume effects caused by clot thickness (Zhu et al., 2023). These limitations highlight the need for more efficient and reliable diagnostic methods.

Recent advancements in clot imaging and artificial intelligence (AI) have significantly improved clot detection and prediction. A systematic review of AI-based and conventional studies (Dumitriu LaGrange et al., 2023) highlighted several key findings. Deep learning (DL) has improved clot detection from non-contrast CT (NCCT) and MRI scans, achieving high sensitivity and specificity in large vessel occlusion (LVO) detection. Radiomics-based models have been developed for clot segmentation and classification, predicting thrombus composition and treatment response using machine learning techniques (Hanning et al., 2021; Hofmeister et al., 2020). Automated clot segmentation is a critical advancement, allowing rapid 3D reconstruction of clots to assist neuroradiologists in identifying clot location, extent, and composition (Mojtahedi et al., 2022). Moreover, AI-based clot detection software, such as MethinksLVO, can rapidly predict the LVO in ischemic stroke patients using the NCCT, reducing diagnostic time and improving early intervention (Olive-Gadea et al., 2020).

Automated detection of stroke characteristics, such as clot location and severity, can significantly enhance diagnostic efficiency. Currently, the SVS detection heavily relies on manual assessment by neurologists, which is time-consuming and subject to variability. The deep learning offers a promising solution by automating detection and improving accuracy. The DL models have demonstrated near-perfect accuracy in various medical applications (Tsochatzidis et al., 2019; Wessels & van der Haar, 2023). Convolutional neural networks (CNNs) have also been used to develop automated systems capable of detecting intracranial clots on non-contrast CT scans, further enhancing early stroke diagnosis. In the study, a Convolutional neural network (CNN) is used to classify input images as either hyperdense middle cerebral artery (MCA) sign (HMCAS)-positive or HMCAS-negative. The CNN, specifically the Xception architecture, is trained on augmented datasets to identify the presence of HMCAS on non-contrast CT scans in patients with acute ischemic stroke. The CNN demonstrated high diagnostic performance with 82.9% sensitivity, 89.7% specificity, and 86.5% accuracy in leave-one-case-out cross-validation. The study highlights the potential of the deep learning methods, like CNNs, to assist in the accurate identification of HMCAS, which is crucial for the management and treatment of acute ischemic stroke (Shinohara et al., 2020).

AI techniques, particularly machine learning, have been utilised to develop models capable of predicting the origin and composition of thrombi using the MRI data. For instance, a study employed gradient echo sequences (GRE) at 3T MRI to train a machine learning model that could predict atrial fibrillation (AF) as the thrombus origin (Chung et al., 2019). Additionally, the AI has been applied to analyse the SVS on the MRI, which is associated with increased red blood cell (RBC) content in the clot (Benson et al., 2021). This analysis aids in predicting the clot's response to treatments such as mechanical thrombectomy.

The AI-based radiomics plays a crucial role by extracting a vast number of quantitative features from the MRI scans to develop predictive models. These models can forecast treatment outcomes, including the likelihood of successful recanalisation and number of thrombectomy passes required (Dumitriu LaGrange et al., 2023). Moreover, the AI can integrate information from multiple MRI sequences to provide a comprehensive assessment of the thrombus and surrounding vascular anatomy, facilitating more informed treatment decisions. Overall, the AI applications in the MRI for clot imaging are transforming the field by enabling more accurate and detailed analyses, ultimately improving treatment planning and outcomes for stroke patients.

The classification of biomedical images, including stroke clot detection, is a substantial challenge due to the limited availability of annotated datasets and high computational cost of training deep learning models from scratch. Transfer learning has emerged as an effective solution, leveraging pre-trained deep learning models to enhance classification accuracy while reducing data requirements (Gunturu et al., 2024). By adapting pre-trained neural networks,

such as ResNet, DenseNet, and VGG, to domain-specific biomedical imaging tasks, the transfer learning significantly improves model performance while shortening training time.

In stroke detection, the transfer learning allows models trained on large general image datasets (e.g., ImageNet) to be fine-tuned on smaller, domain-specific datasets, such as the SWI-based clot images. This approach preserves critical features while requiring fewer labelled images, making it a powerful tool for detecting clots in the MRI scans. Studies have shown that fine-tuning deep convolutional networks on medical images achieves higher accuracy than training models from scratch, especially in cases with limited patient data.

This study aims to develop an automated detection system for the SVS identification in acute ischemic stroke using the transfer learning. To the best of our knowledge, this approach is novel as it integrates the SWI with the DL-based clot detection. The proposed system seeks to enhance stroke diagnosis by ensuring high accuracy and efficiency, leveraging state-of-the-art DL techniques in medical imaging. By incorporating the latest advancements in AI and deep learning, this research contributes to improving stroke detection, treatment planning, and overall patient outcomes.

LITERATURE REVIEW

Machine learning (ML) has recently provided a major breakthrough in the medical sector, particularly in stroke treatment. Diverse data on medicine can be processed by the ML, which, in many cases, identifies patterns and predicts them with astonishing accuracy. The first category pertains to stroke prevention, and the second one belongs to stroke diagnosis, whereas the third one is for treatment of strokes, while the fourth means outcome prediction in case of stroke.

Stroke Prevention

Preventing stroke is necessary to minimise the rates and impact of strokes. The ML techniques have demonstrated the potential for policy definition for risk factors and prediction of stroke-prone conditions. This section discusses research literature that has utilised the ML models to predict familial hypercholesterolemia (FH) and carotid-artery atherosclerosis, which are leading causes of stroke among individuals across the globe (Myers et al., 2019). The FH is an inherited condition that causes high cholesterol and a risk of premature heart disease or stroke. Performing early identification of the FH allows for the performance of health, promoting activities that reduce long-term cardiovascular risk. A study using the random forest (RF) algorithm is one of its notable examples to predict the FH. The method had to optimise the parameters and used a 5-fold cross-validation approach for stability assessment with respect to potential model overfitting. The study performed parameter optimisation and 5-fold cross-validation to ensure that the model has good performance. The precision was 0.85, and the recall was 0.45. Although the high

precision suggests solid performance, sub-performances seem to follow in their shadows, emphasising a possible area of concern. Hence, more effort is required for this model as it appears to be weak with respect to detecting the FH patients. Regardless, it illustrates the possibility of the ML to improve the detection of stroke risk-related genetic conditions, especially the RF. Carotid-artery atherosclerosis (CA), one of the main risk factors for ischemic stroke, represents plaque aggregation in carotids. Early recognition of the CA can lead to preventive management and reduce the risk of strokes. In a study (Bento et al., 2019), a support vector machine (SVM) was trained to classify individuals with the CA based on the MRI images. The SVM model performed with an accuracy of 97.6%, which indicated that the use of this algorithm could help in the identification of high-risk populations. The combination of the MRI images with the SVM results in a non-invasive diagnostic instrument for the CA, which has important clinical implications as it could enable early management and stroke prevention.

Stroke Diagnosis

A more accurate classification of the stroke subtypes, particularly the distinction between the ischemic and hemorrhagic strokes, which has implications for their treatment strategy, could lead to better patient outcomes. In this part, we discuss the results of the previous study of dividing stroke patients into subtypes and predicting outcomes using the ML techniques. In a stroke subtype classification study (Peixoto & Rebouças Filho, 2018), researchers used different ML techniques such as the SVM, Multi-layer Perceptron, and Minimal Learning Machines, together with the standard linear discriminant analysis as well as the structure co-occurrence matrix (SCM).

The objective was to differentiate between the ischemic and hemorrhagic strokes using imaging. Of the evaluated techniques, the SCM achieved the best performance, achieving an accuracy of 98%. This high level of accuracy emphasises the capacity of the SCM to accurately classify sub-types for all stroke types, thus becoming a valuable tool to help health professionals make reliable clinical decisions. For instance, Giacalone et al. (2018) predicted the final lesion for stroke patients with acute ischemic using raw perfusion MRI images. An SVM model is implemented in this study to measure brain stroke lesion extent and location prediction using the MRI data. The SVM model displayed satisfactory high accuracy (95%), and it could be predicted with precision. This type of prediction can be used to support therapeutic decisions or prognosis assessment.

Stroke Treatment

Stroke rehabilitation is a crucial part of treatment to improve physical and cognitive abilities in patients. The ML-based models have been employed to enhance rehabilitation exercises, in particular by utilising physiological signals and sensor technology for

personalised therapy designing and assessment. This section summarises studies that applied the ML techniques to optimise stroke rehabilitation, specifically in the areas of physiological stress identification and upper extremity function improvement. A study that focussed on trying to adapt the rehabilitation therapy to the physiological signals of patients organised this information into relaxed, medium-stressed, and over-stressed (Badesa et al., 2014). The physiological signals were classified using a number of the ML methods, the most significant results achieved by support vector machines with radial basis function (RBF) kernel. The SVM with RBF achieved an accuracy of 91.43%. The high accuracy indicates that the SVM with RBF can reliably interpret physiological signals, allowing the therapist to adjust the intensity and type of rehabilitation exercise in real time, thereby enhancing the effectiveness of the therapy. Another study focussed on improving upper extremity function post-rehabilitation, particularly targeting motor-specific responses. Traditional evaluation approaches, such as self-reporting, are often accurate but subjective (Bochniewicz et al., 2017). By using the sensor technology, accurate and objective data were collected to assess motor function. The study used the RF to classify the rehabilitation outcomes for control and stroke subjects. From the study, while the RF model was highly effective in distinguishing motor responses in healthy individuals, it faced challenges with the more variable and complex data from stroke patients. However, the sensor data and RF classification have greatly advanced beyond the traditional self-report method, whereby a more objective and detailed evaluation of rehabilitation progress may be obtained. Patients with stroke are frequently treated by thrombolysis, thrombectomy, or both and experience a highly variable outcome. Such fine-grained prognostication can help guide the choice of treatments and ultimately improve patient care. The ML techniques have been used with the clinical and imaging data to predict treatment response. In this section, studies are considered in predicting treatment outcomes using the ML and DL methods, especially focussing on the utilisation of the CTA images and diffusion tensor imaging (DTI). A study investigated the use of the DL for predicting functional outcomes after treatment in stroke from acquired computed tomography angiograms (Hilbert et al., 2019). The research employed the Resnet algorithm in order to analyse the CTA images and predict patient outcomes. This method was compared to traditional radiological biomarkers that were manually annotated by domain experts, who can introduce inter-observer variability. On 3 out of 4 cross-validation folds for functional outcomes, the model achieved an average AUC value of 0.71. The study results suggest that, compared with traditional radiological biomarkers, the DL model can more accurately predict outcomes and thus offers hope in improving the administration of stroke treatment. A further study using the ML explored the link between the DTI metrics and functional outcomes in a cohort of patients post-stroke. The axial diffusivity map as a key parameter was the central object of the study.

These maps were analysed, and the results were predicted using an SVM classifier. The SVM classifier had the highest accuracy rate, 82.8%, among imaging criteria in this current study. This result attests to the utility of the DTI metrics and SVM for forecasting outcomes, suggesting an effective approach used for assessing rehabilitation strategies.

Stroke Outcomes Prediction

The thrombus composition and stroke treatment response outcome may be influenced by the thrombotic material within a clot as well as its responsiveness to treatment. Radiomics of the clot, which examines connections between the thrombus composition and treatment response through sophisticated imaging techniques, is in increasing focus. The ML algorithms have demonstrated the potential to predict the composition of the thrombus and recognise specific stroke-related conditions. In this section, we summarise some representative studies that have used the ML for clot imaging in stroke treatment. Another was targeting prediction on the thrombus composition of clots using radiomics features extracted from the thrombi images (Hanning et al., 2021). The investigators applied nested five-fold cross-validation and used random-forest algorithms to classify the thrombus composition. At the end of this process, a receiver operating characteristic (ROC) curve value of 0.83 was obtained for red blood cell (RBC)-rich thrombi and another 0.84 for fibrin-rich thrombi by the random forest model, respectively. The high ROC value showed the random forest model to have differentiation power between the RBC-rich and fibrin-thrombi. Therefore, accurate prediction of the thrombus composition can help guide appropriate treatment strategies.

The identification of the LVO on the NCCT plays a key role in the decision-making process to identify which is going to be the right intervention for stroke patients. The proprietary MethinkLVO software created to aid in this identification had a sensitivity of 0.83 and specificity of 0.71 (Olive-Gadea et al., 2020). High sensitivity (92.7%) and specificity (99.8%) imply that the software is good at detecting the LVO to inform clinical decisions accurately with sufficiently low false discovery rate. A stunning result predicting the hyperdense middle cerebral artery (HMCA) in the NCCT showed the sensitivity and specificity were 0.83 (Xception model) and shown to be effective at HMCA identification, aiding in rapid diagnosis and intervention for acute stroke cases (Shinohara et al., 2020).

The SVS in susceptibility-weighted imaging has been linked with higher amounts of the RBC content within thrombi (Phuyal et al., 2024). A study by Tang et al. (2021) found clots without the SVS were fibrin-rich and less responsive to simple aspiration, requiring mechanical thrombolysis instead. In patients with the LVO treated with intravenous tissue plasminogen activator (TPA) alone, the presence of the SVS has similarly been identified as a predictor for better outcome thresholds (Tang et al., 2021). Although the SVS as a clot composition marker is extremely important, until now, no study has ever focussed on the

automatic detection of this sign based on the ML or DL. These gaps automatically denote an interesting direction in further development.

MATERIALS AND METHODS

This study comprises three main experimental phases. Phase 1 evaluates different pre-trained deep learning models using the Shinohara's method (Shinohara et al., 2020) to determine the best-performing architecture for the SVS detection, incorporating data augmentation. Phase 2 optimises the selected model by analysing the effects of augmentation strategies, learning rate, training epochs, resizing methods, and filtering techniques. Finally, Phase 3 validates the optimal configuration using the 5-fold cross-validation to ensure the generalisability of the developed model.

Experimental Setup

Phase 1: Deep Learning Model Selection

Step 1: Pre-Trained Models Evaluated. In this study, six prominent deep learning architectures were evaluated to identify the most effective model for the susceptibility-weighted Imaging (SWI) MRI scan analysis. The selected architectures are:

- Xception: This architecture utilises depthwise separable convolutions, which significantly reduce the number of parameters without compromising performance. The Xception has demonstrated superior accuracy in various image classification tasks, making it a strong candidate for medical image analysis (Faiz & Iqbal, 2022).
- ResNet50: Known for its residual learning framework, the ResNet50 addresses the vanishing gradient problem by incorporating skip connections. This design enables the training of deeper networks and has shown robust performance across diverse applications (Shen & Liu, 2017).
- DenseNet121: The DenseNet connects each layer to every other layer in a feed-forward fashion, promoting feature reuse and efficient gradient flow. This connectivity pattern leads to improved learning efficiency and has been effective in various computer vision tasks.
- MobileNet: Designed for mobile and embedded vision applications, the MobileNet employs depthwise separable convolutions to reduce computational complexity. Despite its lightweight nature, it achieves performance comparable to larger models, making it suitable for resource-constrained environments (Chen & Su, 2018).
- EfficientNetB0: The EfficientNet introduces a compound scaling method that uniformly scales network depth, width, and resolution. This balanced approach results in superior accuracy with fewer parameters, offering an efficient solution for image classification tasks (Utami et al., 2022).

- ConvNeXtLarge: As a modernised architecture, the ConvNeXtLarge builds upon standard convolutional networks by incorporating design elements from vision transformers. This integration aims to enhance performance while maintaining computational efficiency, making it a compelling choice for advanced image analysis (Hou et al., 2024).

Each of these architectures brings unique strengths to the table, and their performance was systematically evaluated to determine the most suitable model for our specific application.

Step 2: Implementation of the Method Inspired by Shinohara. Each pre-trained model was used as a feature extractor, replacing the final classification layers with a customised classifier. The classification head was designed as follows:

- Global average pooling layer
- Batch normalisation layer
- Dropout layer (0.3)
- Fully connected dense layer with sigmoid activation for binary classification

Step 3: Dataset and Preprocessing. All images with positive SVS are annotated by a neuroradiologist from Hospital Sultan Abdul Aziz Shah (HSAAS), Faculty of Medical and Health Science, Universiti Putra Malaysia (UPM), Malaysia. Data obfuscation, labelling and validation were done using padimedical system. The dataset comprises nine patients who exhibit the susceptibility vessel sign in the SWI MRI scans. Each SWI MRI scan contains 60 2D image slices. However, not all images contain positive signs of the SVS. The number of slices for each patient consisting of the SVS positive also varies. The total number of the SVS-positive images for this experiment is 66. For the training set taken from five patients, 30 images with the SVS positive and 30 images with the SVS negative are used. The validation set includes 19 images with the SVS positive and 19 images with the SVS negative, which is from two patients, while the testing dataset consists of 17 images with the SVS positive and 17 images with the SVS negative sign, which were obtained from another two patients. The images and data obtained initially are in the DICOM format, which is then converted into the JPEG format (672 × 672 pixels). All images with the positive SVS are taken into the dataset. Each full brain image with a SVS positive is cropped into various sizes of squares depending on the area of the SVS, ensuring that the information on the SVS is maximised in the background as shown in Figure 1 (the shape of the cropped area is square and being used as an input of classification), for the SVS negative is taken from the same image but in different position of the SVS positive. If the SVS positive is on the right side of the brain image, the SVS negative is taken from the left side of the brain, as shown in Figure 1. Each dataset (training, validation, and testing) are then organised

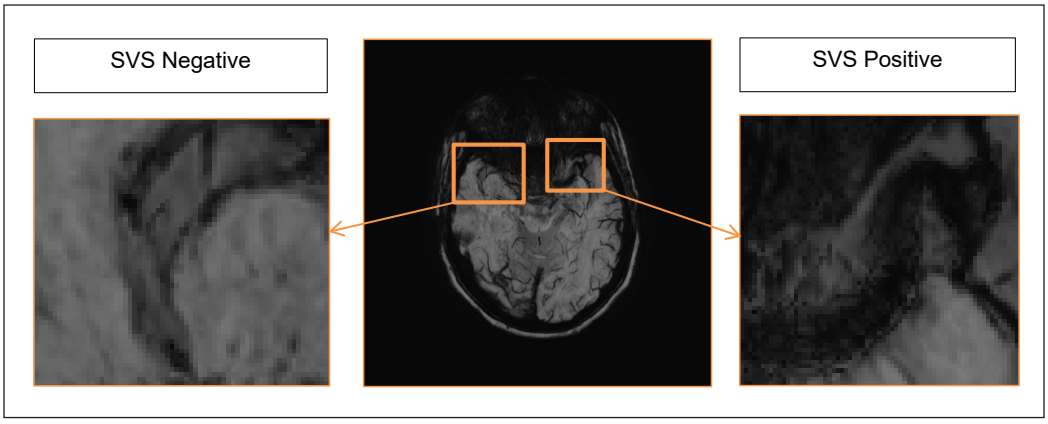

Figure 1. This is one of the image slices taken from acute ischemic stroke patients using the MRI modality with the SVS positive. This image is cropped into the negative SVS region and the positive SVS region that is used during the experiment
Note. MRI = Magnetic resonance imaging; SVS = Susceptibility vessel sign

into separate folders, which are further subdivided into images of the SVS positive and negative. Each of the images was resized to 240 × 240 using bilinear interpolation. Then, the filtering method was applied to reduce the noise. Data augmentation is employed to enable the model to understand various sets of features and expand the dataset size, thus mitigating overfitting. Each training set is augmented using random affine transformation, including shearing and rotation. The details of the image augmentation parameters are as follows: rotation within a range of 0 to 90 degrees in a step of 15 degrees, shearing at 0.2, zooming at 0.2, horizontal flipping, and vertical flipping. From this augmentation method, 300 augmented images were obtained for the training dataset.

Step 4: Model Training Configuration. For this study, each of the pre-trained models used this parameter as shown below:

- Optimiser: Adam with a fixed learning rate of 0.00001
- Batch size: 32
- 50 training epochs
- Loss function: Binary cross-entropy

Step 5: Evaluation Metrics and Model Selection. In this study, a few parameters are used to measure the efficiency and effectiveness of the classification model, using accuracy, sensitivity, and specificity derived from the confusion matrix. The calculation of each performance metric is as follows:

$$\text{Accuracy} = \frac{TP + TN}{TP + FP + TN + FN} \quad [1]$$

$$\text{Sensitivity} = \frac{\text{TP}}{\text{TP} + \text{FN}} \quad [2]$$

$$\text{Specificity} = \frac{\text{TN}}{\text{TN} + \text{FP}} \quad [3]$$

where, TP is true positive, TN is true negative, FP is false positive, and FN is false negative.The pre-trained model achieving the highest F1-score was selected for further experimentation in Phase 2.

Phase 2: Manual Hyperparameter Tuning of the Best Pre-Trained Model

After identifying the best-performing pre-trained model in Phase 1, an optimisation experiment was conducted using a manual hyperparameter tuning to examine the impact of augmentation strategies, learning rates, training epochs, resizing methods, and filtering techniques on the classification performance.

Experimental Configurations. The selected model was fine-tuned under different experimental conditions:

Step 1: Data Augmentation Strategies. The study analysed the impact of data augmentation on model performance by comparing two different training approaches:

1. **With Augmentation** – Various augmentation techniques were applied to enhance model generalisation and robustness. The applied transformations included:
   - Rotation: 0° to 90° with 15° step
   - Shear: 0.2
   - Zoom: 0.2
   - Horizontal and vertical flipping

   These augmentations were consistent with those used in **Phase 1** of the study.
2. **Without Augmentation** – The model was trained using the original dataset without any transformations, serving as a baseline for comparison.

The impact of augmentation was assessed based on model accuracy, generalisation capability, and sensitivity to variations in the input data.

Step 2: Learning Rate Variations (Manually Tuned). The study explored the impact of different manually tuned learning rates on the model performance. The following learning rate variations were tested:

- 10^{-3} (0.001) - A relatively high learning rate, allowing the model to converge quickly but with a potential risk of overshooting the optimal solution.
- 10^{-4} (0.0001) - A moderate learning rate, balancing convergence speed and stability.

- 10^{-6} (0.000001) - A very small learning rate, ensuring fine adjustments to the model's weight but potentially leading to slow convergence.

Step 3: Number of Training Epochs (Manually Tuned). The study investigated the effect of different training durations on the model performance by varying the number of training epochs. The following configurations were tested:

- 25 epochs – A shorter training duration to observe the model's initial learning progress and prevent overfitting.
- 50 epochs – A balanced approach, allowing the model to learn effectively while monitoring for potential overfitting.
- 70 epochs – A longer training duration to evaluate whether extended learning improves performance or leads to overfitting.

Early stopping was implemented based on the validation accuracy to determine the optimal number of epochs for achieving the best generalisation performance on test data.

Step 4: Resizing Methods. The study evaluated different image resizing techniques to determine their impact on model performance. The following interpolation methods were considered:

- Bilinear interpolation – Computes the pixel value using a weighted average of the four nearest neighbouring pixels, resulting in smoother images.
- Bicubic interpolation – Uses a more complex weighted average of 16 neighbouring pixels, producing sharper and higher-quality resized images.
- Nearest neighbour interpolation – Assigns the value of the nearest pixel without averaging, leading to a blocky appearance but preserving edges.

Each method was tested to assess its influence on image quality and the model's ability to detect the SVS effectively.

Step 5: Filtering Techniques. The study explored different image filtering techniques to assess their impact on model performance. The following filtering approaches were evaluated:

- No filtering – The raw images were used without any pre-processing.
- Median filter – Applied to reduce noise while preserving edges.
- Gaussian filter – Used for smoothing the images by reducing high-frequency noise.
- Combination of median and Gaussian filtering – Both techniques were applied sequentially to enhance image quality.

Each filtering method was analysed to determine its effectiveness in improving the model accuracy and generalisation.

Training and Evaluation Process. The Adam optimiser was employed for backpropagation across various manually selected learning rates to optimise the model's performance. Training was conducted for a range of epochs, with early stopping implemented to monitor validation accuracy and prevent overfitting. The best-performing configuration was identified based on the overall accuracy and generalisation performance evaluated on the test dataset.

Selection of the Optimal Configuration. After evaluating all experimental configurations, the optimal combination of augmentation techniques, image resizing, filtering methods, learning rate, and training epochs were selected based on the performance metrics. This final validated model was then subjected to 5-fold cross-validation in Phase 3 to ensure its robustness and generalisation capability.

Phase 3: 5-Fold Cross-Validation on the Optimal Configuration

Once the best model configuration was established, the 5-Fold Cross-validation was employed to validate its generalisability. The 5-Fold Cross-validation Strategy was implemented to evaluate the model's performance robustly. The dataset was randomly divided into five equal folds. In each iteration, one-fold was designated as the validation set, while the remaining four folds were used for training the model. This process was repeated five times, with each fold serving as the validation set exactly once. The final performance of the model was determined by calculating the mean performance across all five folds, providing a more reliable assessment of its generalisation capability.

RESULTS AND DISCUSSION

In this study, the performance of the multiple deep learning models for the detection of the SVS in the MRI scans was evaluated using the method proposed by Shinohara et al. (2020). The models assessed include the Xception, ResNet50, ConvNetXtXLarge, EfficientNet, MobileNet, and DenseNet. The performance of these models was analysed based on key classification metrics: accuracy, sensitivity, and specificity.

The results based on Table 1 indicate that the Xception achieved an accuracy of 52.94%, with a sensitivity of 1.00 and specificity of only 0.05. Similarly, the ResNet50, ConvNetXtXLarge, and EfficientNet all reported an accuracy of 50.00%, a perfect sensitivity score of 1.00, but a specificity of 0.00. This pattern suggests that these models overwhelmingly classified images as positive cases (SVS present), failing to correctly identify negative cases. Consequently, their high sensitivity came at the expense of specificity, making them ineffective for reliable classification in clinical settings. The DenseNet is better than the ResNet because the Densenet has the capability of feature reuse and better gradient flow (Padmakala & Uma Maheswari, 2024).

Table 1
Comparing performance metrics of the transfer learning models in the test dataset

Model	Accuracy	Sensitivity	Specificity
Xception	0.5294	1.00	0.05
ResNet 50	0.5000	1.00	0.00
ConvNetXtXLarge	0.5000	1.00	0.00
EfficientNetB0	0.5000	1.00	0.00
MobileNet	0.5588	0.7647	0.3529
DenseNet121	**0.5882**	**0.7647**	**0.4818**

Note. The bold data = The best results

The MobileNet demonstrated a relatively improved performance, achieving an accuracy of 55.88%, sensitivity of 0.7647, and specificity of 0.3529. Likewise, the DenseNet outperformed the other models by achieving the highest accuracy of 58.82%, with a sensitivity of 0.7647, and a specificity of 0.4818. These models showed a better balance between sensitivity and specificity, indicating that they were more capable of distinguishing between positive and negative cases than the other models. The Densenet model also shows outperformed in brain tumour detection because it is capable of handling small datasets compared to other models (Thimma Reddy & Balaram, 2024). The Densenet pre-trained model has also shown improvement in accuracy in the fundus medical images (Xu et al., 2018), breast cancer detection (Hamdy et al., 2021), chest disease (Iswahyudi et al., 2024), and others.

The results presented in Table 1 indicate that the Xception achieved an accuracy of 52.94%, with a sensitivity of 1.00 but a specificity of only 0.05. Similarly, the ResNet50, ConvNeXt-XLarge, and EfficientNet all reported an accuracy of 50.00%, a perfect sensitivity score of 1.00, but a specificity of 0.00. This pattern suggests that these models overwhelmingly classified images as positive cases (SVS present), failing to correctly identify negative cases. Consequently, their high sensitivity came at the expense of specificity, making them ineffective for reliable classification in clinical settings. The DenseNet outperforms the ResNet due to its ability to facilitate feature reuse and improve gradient flow (Padmakala & Uma Maheswari, 2024).

The MobileNet demonstrated relatively improved performance, achieving an accuracy of 55.88%, a sensitivity of 0.7647, and specificity of 0.3529. Likewise, the DenseNet outperformed the other models by achieving the highest accuracy of 58.82%, with a sensitivity of 0.7647, and specificity of 0.4818. These models exhibited a better balance between sensitivity and specificity, indicating that they were more effective in distinguishing between the positive and negative cases compared to the other models.

After that, in Phase 2, several experiments were conducted to compare the performance of the models with and without data augmentation, as well as to evaluate different resizing,

filtering methods, and other transfer learning models, as mentioned in Phase 2 in the methodology section. In Table 2, the results for without data augmentation are presented, comparing various learning rates and numbers of epochs. Our findings indicate that the best performance was achieved with a learning rate of 0.001 and 50 epochs, yielding an accuracy of 0.8235, with a specificity of 0.8235, a sensitivity of 0.8235, and a F1-score of 0.8235.

Then, performance improvement was observed after using the data augmentation method. As shown in Table 3, the highest performance in that case was achieved with a learning rate of 0.001 and 50 epochs, yielding an accuracy of 0.8824, with a specificity of 0.7647, sensitivity of 1.00, and F1-score of 0.8867.

Next, various resizing methods were evaluated using a learning rate of 0.001 and 50 epochs. The results in Table 4 indicate that bicubic interpolation achieved the highest accuracy of 0.8235 among the resizing methods. Nevertheless, when compared with the results from Table 3 (without any resizing), the performance without resizing was superior.

Furthermore, different filtering methods were compared. Table 5 shows that the best results were obtained without any filtering, achieving an accuracy of 0.7647, while the combination of the median and Gaussian filtering produced the lowest accuracy of 0.5.

In conclusion, the best model is the DenseNet121 model with data augmentation, with a learning rate of 0.001 and a number of epochs of 50. The DenseNet121 model obtained an average accuracy of 0.9464 when evaluated using the 5-Fold Cross-validation, as shown in Table 6. It also showed excellent sensitivity, specificity, and F1-score. The strong F1-score suggests that the model maintains a good balance between sensitivity and specificity, making it highly suitable for the SVS detection, which is supported by a value of a high AUC of 0.9728, shown in Figure 2.

Table 2
Comparing performance metrics of the DenseNet121 Model without augmentation with different learning rates (0.000001,0.00001, 0.001) and several epochs (25,50,70) in the test dataset

Learning rate	Epoch	Accuracy	Sensitivity	Specificity	F1-Score
0.000001	25	0.4706	0.8824	0.0588	0.625
0.000001	50	0.4118	0.1176	0.7059	0.1667
0.000001	70	0.5	0.1176	0.8824	0.1905
0.0001	25	0.6765	0.3529	1	0.5217
0.0001	50	0.5882	0.5882	0.5882	0.5882
0.0001	70	0.4412	0.1765	0.7059	0.24
0.001	25	**0.8235**	**0.8235**	**0.8235**	**0.8235**
0.001	50	0.6765	0.8824	0.4706	0.7317
0.001	70	0.7059	0.7647	0.6471	0.7222
0.000001	25	0.4706	0.8824	0.0588	0.625

Note. The bold data = The best results

Table 3
Comparing performance metrics of the DenseNet121 Model with augmentation with different learning rates (0.000001,0.00001, 0.001) and a number of epochs (25,50,70) in the test dataset

Learning rate	Epoch	Accuracy	Sensitivity	Specificity	F1-score
0.000001	25	0.3529	0.4074	0.6471	0.5
0.000001	50	0.4706	0.2353	0.7059	0.3077
0.000001	70	0.5882	0.8	0.2353	0.3636
0.0001	25	0.7353	0.8235	0.6471	0.767
0.0001	50	0.6176	0.3529	0.8824	0.48
0.0001	70	0.7647	0.6471	0.8824	0.7333
0.001	25	0.7941	0.8235	0.7647	0.8
0.001	**50**	**0.8824**	**0.7647**	**1**	**0.8667**
0.001	70	0.7647	0.7059	0.8235	0.75

Note. The bold data = The best results

Table 4
Comparing performance metrics of the DenseNet Model with augmentation among different resizing methods (bilinear, nearest, and bicubic) with a learning rate of 0.001 and the number of epochs of 50 in the test dataset

Resize method	Epoch	Accuracy	Sensitivity	Specificity	F1-score
Bilinear	50	0.7353	0.7647	0.7059	0.7429
Nearest	50	0.7059	0.6471	**0.7647**	0.6875
Bicubic	50	**0.8235**	**0.9412**	0.7059	**0.8421**

Note. The bold data = The best results

Table 5
Comparing performance metrics of the DenseNet121 Model with augmentation among different filtering methods (non-filtering, median, Gaussian, and median + Gaussian) with a learning rate of 0.001 and a number of epochs of 70 in the test dataset

Filtering method	Resize	Accuracy	Sensitivity	Specificity	F1-score
None	**None**	**0.7647**	**0.7647**	**0.7647**	**0.7647**
Gaussian	None	0.7059	0.7647	0.6471	0.7222
Median	None	0.7353	0.7059	0.7647	0.7273
Both	None	0.5	0	1	0

Note. The bold data = The best results

Table 6
Cross-validation using 5-fold cross-validation for the best model, the DenseNet121 with data augmentation, the learning rate is 0.001, and the number of epochs is 50

Transfer learning model	Avg. accuracy	Avg. sensitivity	Avg. specificity	Avg. F1-score
DenseNet	0.9464 ± .0393	0.9692 ± 0.0377	0.9231 ± .0487	0.9481 ± .0383

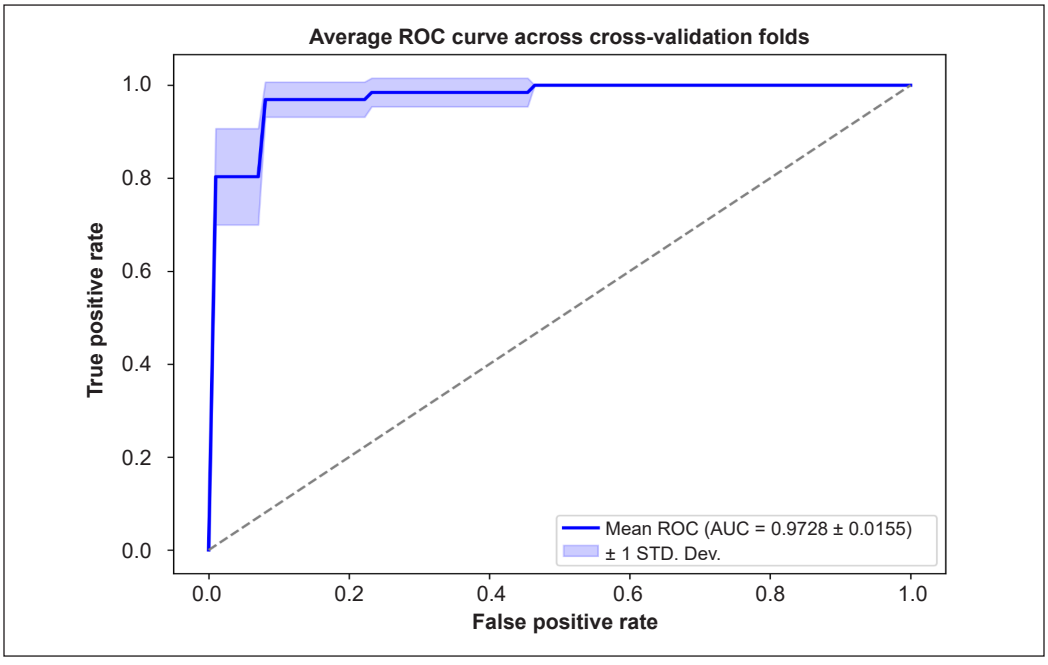

Figure 2. Receiver operating characteristic (ROC) curve in the test dataset using the best model-DenseNet121

CONCLUSION

This study presents the development of a deep learning model for the interactive identification of the SVS in brain stroke patients using the MRI data. A pre-trained DenseNet121 model was fine-tuned with augmented samples and trained using a learning rate of 0.001 for 50 epochs. Experimental results indicate that the data augmentation significantly improved the model performance, whereas image filtering techniques (e.g., median and Gaussian filters) did not yield further enhancement. These findings highlight the effectiveness of the augmentation in enhancing the SVS detection accuracy.

A comparative analysis of the ResNet50 and ConvNeXtXLarge revealed a significant discrepancy in classification performance. Both models achieved 100% sensitivity but 0% specificity, meaning they correctly identified all the SVS-positive cases but failed to classify the SVS-negative cases accurately. This suggests severe overfitting, where the models memorised features from the SVS-positive class rather than learning generalisable patterns. Several factors may have contributed to this issue, including the small dataset size, the complexity of the models, and insufficient regularisation.

The AUC score further confirms the model's strong classification ability. The DenseNet121 model achieved an AUC of 0.9728 (Figure 1), indicating excellent discriminative performance. However, despite this high AUC value, a meaningful comparison with human radiologists and existing AI-based stroke detection tools is

necessary to assess its clinical relevance. Additionally, external validation on independent datasets is required to ensure generalisability and robustness in real-world applications.

Furthermore, the DenseNet has also shown superior performance in brain tumour detection, as it is capable of handling small datasets more effectively than other models (Thimma Reddy & Balaram, 2024). Additionally, the DenseNet pre-trained model has demonstrated improved accuracy in various medical imaging applications, including fundus images (Xu et al., 2018), breast cancer detection (Hamdy et al., 2021), and chest disease diagnosis (Iswahyudi et al., 2024), among others.

Our study addresses the challenges posed by limited radiology data through employing the transfer learning, image augmentation, and various pre-processing techniques. Nevertheless, some limitations must be considered. The samples were extracted from a small region and manually delineated, whereas an automatic approach would be preferable. Additionally, the limited dataset size and potential data variability or class imbalance may have contributed to overfitting.

For future work, our approach is planned to be refined by developing an automatic segmentation method, improving accuracy through hyperparameter tuning, and exploring alternative strategies to enhance the model's robustness and generalisation performance. Furthermore, a comparative study with radiologists and existing AI models will be conducted to evaluate its clinical applicability and real-world effectiveness.

ACKNOWLEDGEMENTS

We would like to thank the radiology team at HSAAS, UPM, Malaysia, for their support in image annotation and clinical insights. We also acknowledge the Centre for Intelligent Signal and Imaging Research (CISIR), Universiti Teknologi PETRONAS (UTP), for their technical guidance and support throughout this study.

REFERENCES

Badesa, F. J., Morales, R., Garcia-Aracil, N., Sabater, J. M., Casals, A., & Zollo, L. (2014). Auto-adaptive robot-aided therapy using machine learning techniques. *Computer Methods and Programs in Biomedicine*, *116*(2), 123–130. https://doi.org/10.1016/j.cmpb.2013.09.011

Benson, J. C., Kallmes, D. F., Larson, A. S., & Brinjikji, W. (2021). Radiology-pathology correlations of intracranial clots: Current theories, clinical applications, and future directions. *American Journal of Neuroradiology*, *42*(9), 1558–1565. https://doi.org/10.3174/ajnr.A7249

Bento, M., Souza, R., Salluzzi, M., Rittner, L., Zhang, Y., & Frayne, R. (2019). Automatic identification of atherosclerosis subjects in a heterogeneous MR brain imaging data set. *Magnetic Resonance Imaging*, *62*, 18–27. https://doi.org/10.1016/j.mri.2019.06.007

Bochniewicz, E. M., Emmer, G., McLeod, A., Barth, J., Dromerick, A. W., & Lum, P. (2017). Measuring functional arm movement after stroke using a single wrist-worn sensor and machine learning.

Journal of Stroke and Cerebrovascular Diseases, *26*(12), 2880–2887. https://doi.org/10.1016/j.jstrokecerebrovasdis.2017.07.004

Chen, H.-Y., & Su, C.-Y. (2018). An enhanced hybrid MobileNet. In *9th International Conference on Awareness Science and Technology* (pp. 308–312). IEEE. https://doi.org/10.1109/ICAwST.2018.8517177

Chung, J. -W., Kim, Y. -C., Cha, J., Choi, E. -H., Kim, B. M., Seo, W. -K., Kim, G. -M, & Bang, O. Y. (2019). Characterization of clot composition in acute cerebral infarct using machine learning techniques. *Annals of Clinical and Translational Neurology*, *6*(4), 739–747. https://doi.org/10.1002/acn3.751

Dumitriu LaGrange, D., Hofmeister, J., Rosi, A., Vargas, M. I., Wanke, I., Machi, P., & Lövblad, K. -O. (2023). Predictive value of clot imaging in acute ischemic stroke: A systematic review of artificial intelligence and conventional studies. *Neuroscience Informatics*, *3*(1), 100114. https://doi.org/10.1016/j.neuri.2022.100114

Faiz, M. F. I., & Iqbal, M. Z. (2022). XceptionUnetV1: A lightweight DCNN for biomedical image segmentation. In L. Barolli, F. Hussain, & T. Enokido (Eds.), *Advanced information networking and applications* (pp. 23–32). Springer. https://doi.org/10.1007/978-3-030-99619-2_3

Giacalone, M., Rasti, P., Debs, N., Frindel, C., Cho, T. -H., Grenier, E., & Rousseau, D. (2018). Local spatio-temporal encoding of raw perfusion MRI for the prediction of the final lesion in stroke. *Medical Image Analysis*, *50*, 117–126. https://doi.org/10.1016/j.media.2018.08.008

Gunturu, V., Maiti, N., Toure, B., Kunekar, P., Banu, S. B., & Lenin, D. S. (2024). Transfer learning in biomedical image classification. In *International Conference on Advances in Computing, Communication and Applied Informatics* (pp. 1–5). IEEE. https://doi.org/10.1109/accai61061.2024.10601862

Hamdy, E., Zaghloul, M. S., & Badawy, O. (2021). Deep learning supported breast cancer classification with multi-modal image fusion. In *22nd International Arab Conference on Information Technology* (pp. 1–7). IEEE. https://doi.org/10.1109/ACIT53391.2021.9677099

Hanning, U., Sporns, P. B., Psychogios, M. N., Jeibmann, A., Minnerup, J., Gelderblom, M., Schulte, K., Nawabi, J., Broocks, G., Meyer, L., Krähling, H., Brehm, A., Wildgruber, M., Fiehler, J., & Kniep, H. (2021). Imaging-based prediction of histological clot composition from admission CT imaging. *Journal of Neurointerventional Surgery*, *13*(11), 1053–1057. https://doi.org/10.1136/neurintsurg-2020-016774

Hilbert, A., Ramos, L. A., van Os, H. J. A., Olabarriaga, S. D., Tolhuisen, M. L., Wermer, M. J. H., Barros, R. S., van der Schaaf, I., Dippel, D., Roos, Y. B. W. E. M., van Zwam, W. H., Yoo, A. J., Emmer, B. J., Lycklama à Nijeholt, G. J., Zwinderman, A. H., Strijkers, G. J., Majoie, C. B. L. M., & Marquering, H. A. (2019). Data-efficient deep learning of radiological image data for outcome prediction after endovascular treatment of patients with acute ischemic stroke. *Computers in Biology and Medicine*, *115*, 103516. https://doi.org/10.1016/j.compbiomed.2019.103516

Hofmeister, J., Bernava, G., Rosi, A., Vargas, M. I., Carrera, E., Montet, X., Burgermeister, S., Poletti, P. -A., Platon, A., Lovblad, K. -O., & MacHi, P. (2020). Clot-based radiomics predict a mechanical thrombectomy strategy for successful recanalization in acute ischemic stroke. *Stroke*, *51*(8), 2488-2494. https://doi.org/10.1161/STROKEAHA.120.030334

Hou, Q., Lu, C. -Z., Cheng, M. -M., & Feng, J. (2024). Conv2Former: A simple transformer-style ConvNet for visual recognition. In *IEEE Transactions on Pattern Analysis and Machine Intelligence* (Vol 46, No. 12, pp. 8274–8283). IEEE. https://doi.org/10.1109/TPAMI.2024.3401450

Iswahyudi, W., Farhan Ali Irfani, M., Dwi Mahandi, Y., Ari Elbaith Zaeni, I., Sendari, S., & Widiyaningtyas, T. (2024). Analyzing the effectiveness of MobileNetV2, Xception, and DenseNet for classifying chest diseases: Pneumonia, pneumothorax, and cardiomegaly. In *International Conference on Electrical Engineering and Computer Science* (pp. 251–255). IEEE. https://doi.org/10.1109/ICECOS63900.2024.10791269

Mojtahedi, M., Kappelhof, M., Ponomareva, E., Tolhuisen, M., Jansen, I., Bruggeman, A. A. E., Dutra, B. G., Yo, L., LeCouffe, N., Hoving, J. W., van Voorst, H., Brouwer, J., Terreros, N. A., Konduri, P., Meijer, F. J. A., Appelman, A., Treurniet, K. M., Coutinho, J. M., Roos, Y., van Zwam, W., … Marquering, H. (2022). Fully automated thrombus segmentation on CT images of patients with acute ischemic stroke. *Diagnostics*, *12*(3), 698. https://doi.org/10.3390/diagnostics12030698

Myers, K. D., Knowles, J. W., Staszak, D., Shapiro, M. D., Howard, W., Yadava, M., Zuzick, D., Williamson, L., Shah, N. H., Banda, J. M., Leader, J., Cromwell, W. C., Trautman, E., Murray, M. F., Baum, S. J., Myers, S., Gidding, S. S., Wilemon, K., & Rader, D. J. (2019). Precision screening for familial hypercholesterolaemia: A machine learning study applied to electronic health encounter data. *The Lancet Digital Health*, *1*(8), e393–e402. https://doi.org/10.1016/S2589-7500(19)30150-5

Olive-Gadea, M., Crespo, C., Granes, C., Hernandez-Perez, M., Pérez de la Ossa, N., Laredo, C., Urra, X., Carlos Soler, J., Soler, A., Puyalto, P., Cuadras, P., Marti, C., & Ribo, M. (2020). Deep learning based software to identify large vessel occlusion on noncontrast computed tomography. *Stroke*, *51*(10), 3133–3137. https://doi.org/10.1161/STROKEAHA.120.030326

Padmakala, S., & Uma Maheswari, S. (2024). Deep learning-based MRI analysis for brain tumor detection: Insights from ResNet and DenseNet models. In *8th International Conference on Electronics, Communication and Aerospace Technology* (pp. 1620–1626). IEEE. https://doi.org/10.1109/ICECA63461.2024.10800894

Peixoto, S. A., & Rebouças Filho, P. P. (2018). Neurologist-level classification of stroke using a Structural Co-Occurrence Matrix based on the frequency domain. *Computers and Electrical Engineering*, *71*, 398–407. https://doi.org/10.1016/j.compeleceng.2018.07.051

Phuyal, S., Paudel, S., Chhetri, S. T., Phuyal, P., Shrestha, S., & Maharjan, A. M. S. (2024). Susceptibility weighted imaging for detection of thrombus in acute ischemic stroke: A cross-sectional study. *Health Science Reports*, *7*(8), e2285. https://doi.org/10.1002/hsr2.2285

Shen, Z., & Liu, Y. (2017). A novel connectivity of deep convolutional neural networks. In *Chinese Automation Congress* (pp. 7779–7783). IEEE. https://doi.org/10.1109/CAC.2017.8244187

Shinohara, Y., Takahashi, N., Lee, Y., Ohmura, T., & Kinoshita, T. (2020). Development of a deep learning model to identify hyperdense MCA sign in patients with acute ischemic stroke. *Japanese Journal of Radiology*, *38*(2), 112–117. https://doi.org/10.1007/s11604-019-00894-4

Sirsat, M. S., Fermé, E., & Câmara, J. (2020). Machine learning brain stroke: A review. *Journal of Stroke and Cerebrovascular Diseases*, *29*(10), 105162. https://doi.org/10.1016/j.jstrokecerebrovasdis.2020.105162

Tang, S. Z., Sen, J., Goh, Y. G., & Anil, G. (2021). Susceptibility vessel sign as a predictor for recanalization and clinical outcome in acute ischaemic stroke: A systematic review and meta-analysis. *Journal of Clinical Neuroscience*, *94*, 159–165. https://doi.org/10.1016/j.jocn.2021.10.017

Thimma Reddy, B., & Balaram, V. V. S. S. S. (2024). MAFD: Model Agnostic Forest Densenet Approach for brain tumor detection. In R. R. Chillarige, S. Distefano, & S. S. Rawat (Eds.), *Advances in computational intelligence informatics* (pp. 295–306). Springer. https://doi.org/10.1007/978-981-97-4727-6_30

Tsochatzidis, L., Costaridou, L., & Pratikakis, I. (2019). deep learning for breast cancer diagnosis from mammograms—A comparative study. *Journal of Imaging*, *5*(3), 37. https://doi.org/10.3390/jimaging5030037

Utami, P., Hartanto, R., & Soesanti, I. (2022). The EfficientNet performance for facial expressions recognition. In *5th International Seminar on Research of Information Technology and Intelligent Systems* (pp. 756–762). IEEE. https://doi.org/10.1109/ISRITI56927.2022.10053007

Wessels, S., & van der Haar, D. (2023). Using a genetic algorithm to update convolutional neural networks for abnormality classification in mammography. In *Proceedings of the 12th International Conference on Pattern Recognition Applications and Methods* (pp. 790–797). SciTePress. https://doi.org/10.5220/0011648500003411

Xu, X., Lin, J., Tao, Y., & Wang, X. (2018). An improved DenseNet method based on transfer learning for fundus medical images. In *2018 7th International Conference on Digital Home* (pp. 137–140). IEEE. https://doi.org/10.1109/ICDH.2018.00033

Zhu, K., Bala, F., Zhang, J., Benali, F., Cimflová, P., Kim, B. J., McDonough, R., Singh, N., Hill, M. D., Goyal, M., Demchuk, A., Menon, B. K., & Qiu, W. (2023). Automated segmentation of intracranial thrombus on NCCT and CTA in patients with acute ischemic stroke using a coarse-to-fine deep learning model. *American Journal of Neuroradiology*, *44*(6), 641–648. https://doi.org/10.3174/ajnr.a7878